A unified clumped isotope thermometer calibration (0.5–1100°C) using carbonate-based standardization

N.T. Anderson[1]*, J.R. Kelson[2], S. Kele[3], M. Daëron[4], M. Bonifacie[5], J. Horita[6], T.J. Mackey[7], C.M. John[8], T. Kluge[9], P. Petschnig[11], A.B. Jost[1], K.W. Huntington[10], S.M. Bernasconi[11], K.D. Bergmann[1]

[1]Department of Earth, Atmospheric, and Planetary Sciences, Massachusetts Institute of Technology, Cambridge, MA, 02135

[2]Department of Earth and Environmental Sciences, University of Michigan, Ann Arbor, MI 48109

[3]Institute for Geological and Geochemical Research, Research Centre for Astronomy and Earth Sciences, 1112 Budapest, Hungary

[4]Laboratoire des Sciences du Climat et de lEnvironnement, LSCE/IPSL, CEA-CNRS-UVSQ, Université Paris-Saclay, Orme des Merisiers, F-91191, Gif-sur-Yvette Cedex, France

[5]Université de Paris, Institut de Physique du Globe de Paris, CNRS, F-75005 Paris, France

[6]Department of Geosciences, Texas Tech University, Lubbock, TX, 79409

[7]Department of Earth and Planetary Sciences, University of New Mexico, Albuquerque, NM, 87131

[8]Department of Earth Science and Engineering, Imperial College, Prince Consort Rd, London SW7 2AZ

[9]Institute of Applied Geosciences, Karlsruhe Institute of Technology, Adenauerring 20b, 76131 Karlsruhe, Germany

[10]Department of Earth and Space Sciences and Quaternary Research Center, University of Washington, Seattle, WA, USA

[11]Department of Earth Sciences, ETH Zürich, CH8092, Switzerland

Key Points:

- Reanalysis of previous Δ_{47} calibration samples reconciles their discrepancies.
- No statistically significant difference is observed across a wide range of temperature and sample character.
- This Δ_{47} calibration is near-identical to recent calcite calibrations using carbonate-based standardization.

*77 Massachusetts Ave., Cambridge, MA 02139

Corresponding author: N.T. Anderson, `nanderso@mit.edu`

–1–

Abstract

The potential for carbonate clumped isotope thermometry to independently constrain both the formation temperature of carbonate minerals and fluid oxygen isotope composition allows insight into long-standing questions in the Earth sciences, but remaining discrepancies between calibration schemes hamper interpretation of temperature measurements. To address discrepancies between calibrations, we designed and analyzed a sample suite (41 total samples) with broad applicability across the geosciences, with an exceptionally wide range of formation temperatures, precipitation methods, and mineralogies. We see no statistically significant offset between sample types, although comparison of calcite and dolomite remains inconclusive. When data are reduced identically, the regression defined by this study is nearly identical to that defined by four previous calibration studies that used carbonate-based standardization; we combine these data to present a composite carbonate-standardized regression equation. Agreement across a wide range of temperature and sample types demonstrates a unified, broadly applicable clumped isotope thermometer calibration.

Plain Language Summary

Carbonate clumped isotope thermometry is a geochemical tool used to determine the formation temperature of carbonate minerals. In contrast to previous carbonate thermometers, clumped isotope thermometry requires no assumptions about the isotopic composition of the fluid from which the carbonate precipitated. By measuring the clumped isotope composition (Δ_{47}) of carbonate minerals with a known formation temperature, we can construct an empirical calibration for the clumped isotope thermometer that is necessary to convert from a Δ_{47} value to formation temperature. Many previous studies have created Δ_{47} temperature calibrations, but differences between calibrations have led to large uncertainty in final Δ_{47} temperatures. This study measures a large number of samples that span a wide range of temperature (0.5–1100°C) and include many different types of carbonates. These data show that a single calibration equation can describe many sample types, and that when data are carefully standardized to a common set of carbonate materials, calibrations performed at different laboratories agree almost identically. We combine these data to present a carbonate clumped isotope thermometer calibration with broad applicability across the geosciences.

1 Introduction

Carbonate clumped isotope thermometry is a powerful geochemical tool that can determine the formation temperature of a carbonate mineral based on the temperature-dependent propensity for ^{13}C-^{18}O bond formation in the carbonate crystal lattice (Schauble et al., 2006). By reacting carbonate minerals with acid and measuring the resultant quantity of mass-47 CO_2 molecules (δ^{47}; a value primarily controlled by the abundance of ^{13}C-^{18}O-^{16}O in the analyzed CO_2) and comparing it to a stochastic distribution of mass-47 CO_2 with the same "bulk" isotopic composition ($\delta^{18}O$, $\delta^{13}C$), the excess abundance of the doubly substituted isotopologue (Δ_{47}) can be calculated (Ghosh et al., 2006; Schauble et al., 2006). Because Δ_{47} reflects an internal state of isotope distribution within the carbonate mineral phase, it can be used to calculate mineral formation temperature ($T_{\Delta_{47}}$) as well as the $\delta^{18}O$ of the precipitating fluid. This duo can be leveraged to inform long-standing questions across many geoscience disciplines, including the temperature history of the Earth's oceans, terrestrial paleotemperature, diagenetic history of carbonates, and, when coupled to chronology proxies, basin thermochronology (Finnegan et al., 2011; Snell et al., 2013; Winkelstern & Lohmann, 2016; Lloyd et al., 2017; Mangenot et al., 2018).

The calibration between Δ_{47} and carbonate mineral formation temperature is a key intermediary between measurement of CO_2 gas on a mass spectrometer and calculation of $T_{\Delta_{47}}$. Many laboratories have produced T-Δ_{47} calibrations since the initial study of Ghosh et al. (2006), spanning various temperatures, mineralogies, precipitation methods, analytical techniques, and data processing procedures (e.g., Ghosh et al., 2006; Huntington et al., 2009; Dennis et al., 2011; Kele et al., 2015; Kelson et al., 2017; Bonifacie et al., 2017; Bernasconi et al., 2018; Jautzy et al., 2020). While early attempts to compare empirical calibration studies across laboratories yielded large discrepancies (e.g., Ghosh et al., 2006; Dennis & Schrag, 2010), recent calibration studies have converged on statistically similar slopes for the T-Δ_{47} regression line when data is reduced consistently (Petersen et al., 2019). The convergence of these calibrations is promising, but current discrepancies between empirical calibration equations still lead to $T_{\Delta_{47}}$ differences of ~10 °C for carbonates near Earth surface temperatures and tens of °C for higher temperature samples (Fig. 1; Petersen et al., 2019; Jautzy et al., 2020). Uncertainty from calibrations on this order compounds with analytical uncertainty and hampers interpretation of clumped isotope data.

The source of discrepancy between calibration efforts remains unclear. By reprocessing past calibration data with a consistent data reduction scheme and IUPAC parameter set (Brand et al., 2010; Daëron et al., 2016; Schauer et al., 2016), Petersen et al. (2019) reduced but did not eliminate differences between calibrations. Remaining offset in calibration schemes was attributed to one or more of the following: carbon dioxide equilibrium scale (CDES) standardization scheme (heated/equilibrated gas vs. carbonate-based standardization; number, composition, and distribution of standards), differences in the concentration, temperature, and application method of orthophosphoric acid, sample gas purification procedures, mass spectrometer methods, pressure baseline correction, and kinetic isotope effects during carbonate precipitation (Petersen et al., 2019).

The 'InterCarb' carbonate clumped isotope inter-laboratory comparison project, following the principle of equal sample/standard treatment, demonstrated that using carbonate standards (as opposed to heated/equilibrated gases) to project raw Δ_{47} values into the 'I-CDES' scale yields reproducibility between 25 laboratories neither greater nor smaller than predicted based on fully propagating intra-laboratory analytical uncertainties (Bernasconi et al., submitted; Daëron, submitted). Furthermore, the InterCarb study found that Δ_{47} values of measured carbonate standards are statistically indistinguishable irrespective of procedural differences between laboratories such as sample gas purification, mass spectrometer type, or sample acidification procedure. Jautzy et al. (2020) created a new calibration spanning 5–726°C using carbonate-based standardization, and found the regression equation defined by the data was statistically indistinguishable from a series of previous calibration efforts using carbonate-based standardization (Peral et al., 2018; Bernasconi et al., 2018; Breitenbach et al., 2018; Piasecki et al., 2019; Daëron et al., 2019; Meinicke et al., 2020). Together, these studies support that varying preparation and measurement procedures between laboratories produce consistent results if data are standardized using common carbonate reference materials.

Given the promising inter-laboratory consistency of the InterCarb project (Bernasconi et al., submitted), a new calibration encompassing a spectrum of carbonates relevant to geoscience researchers that is firmly anchored to the I-CDES using carbonate-based standardization is required. To ensure that this calibration is applicable across a wide range of sample material, we reanalyzed a sample suite consisting of natural and synthetic samples measured from four previously discrepant calibration efforts (Kele et al., 2015; Kluge et al., 2015; Bonifacie et al., 2017; Kelson et al., 2017) and analyzed a new suite of low-

–4–

124 temperature lacustrine carbonates from the Dry Valleys, Antarctica and experimentally

125 heated carbonate standards. This sample suite spans broad ranges in temperature (0.5

126 – 1100°C), precipitation method (active degassing, passive degassing, mixed solution, nat-

127 ural precipitation), mineralogy (calcite, dolomite, and minor aragonite), and initial bulk

128 isotopic composition. In accordance with the suggestions of the InterCarb project, the

129 latest anchor values for carbonate standards (ETH-1–4, MERCK, IAEA-C2) were used

130 for carbonate-based standardization, measurement of each sample was replicated at least

131 six times (mean = 9), sample to standard ratio was 1:1, IUPAC parameters were used

132 to correct raw data, and analytical uncertainty and uncertainty associated with creation

133 of the reference frame was propagated throughout. We compare the regression derived

134 from data presented here to a suite of previous studies using carbonate-based standard-

135 ization (recalculated with InterCarb anchor values), and combine these datasets to pro-

136 pose a unified and broadly applicable clumped isotope thermometer calibration.

2 Materials and Methods

2.1 Sample collection and preparation

139 A total of 41 carbonate samples with known precipitation temperatures from four

140 previous calibration efforts (Kele et al., 2015; Kluge et al., 2015; Bonifacie et al., 2017;

141 Kelson et al., 2017), a suite of Antarctic lacustrine carbonate, and a suite of experimen-

142 tally heated ETH standards were (re)analyzed in this study. Sample formation temper-

143 ature ranges from 0.5–1100°C. Three samples are stoichiometric dolomite, one sample

144 is non-stoichiometric proto-dolomite, one sample is aragonite (with minor calcite) and

145 the remainder are calcite (five with minor aragonite; one with minor goethite).

2.1.1 Natural precipitates

147 Six calcite samples were collected from three perenially ice-covered lakes in the Dry

148 Valleys region of Antarctica: two from Lake Fryxell (see Jungblut et al., 2016), three from

149 Lake Joyce (see Mackey et al., 2018), and one from Lake Vanda (see Mackey et al., 2017).

150 These carbonates precipitated in association with microbial mats and are shown by pre-

151 vious work to have extremely low $\delta^{18}O$ values of −30 to −40‰ (Mackey et al., 2018).

Ten tufa and travertine deposits were sampled from central Italy, Hungary, Yunnan Province (China), Yellowstone (USA), and Tenerife (Spain). Detailed description of sample localities and strategy are given in Kele et al. (2015) and references therein.

2.1.2 Laboratory precipitates

Aliquots of ETH-1 (Carrara marble) and ETH-2 (synthetic carbonate) were heated to 1100°C and pressurized to 2000 bar for a period of 24 hours at the ETH Zürich Cold Seal Pressure Vessel Laboratory. Following heating, samples were quenched to room temperature within seconds. See Text S1 in the supporting information for full methods.

Fifteen calcite samples from Kelson et al. (2017) were either precipitated with solutions of $NaHCO_3$ and $CaCl_2$ or by dissolving $CaCO_3$ in H_2O with low pH from CO_2 bubbling, and then inducing precipitation either through N_2 bubbling or passive degassing. Carbonic anhydrase was added to four samples. Temperature precision was ±0.5°C.

Two calcite samples from Kluge et al. (2015) were precipitated by dissolving $CaCO_3$ in H_2O and letting the solution equilibrate for 2–15 hours, filtering out undissolved carbonate, and bubbling N_2 through the solution.

Four (proto)dolomite samples used in this study were originally described in Horita (2014) and Bonifacie et al. (2017). The 80°C sample was precipitated by mixing $MgSO_4$, $Ca(NO_3)_4H_2O$, and Na_2CO_3 in a sealed glass bottle for 41 days. The 100, 250, and 350°C samples were made by mixing ground natural aragonite or calcite with a Ca-Mg-(Na)-Cl solution and held within 2°C of prescribed value for 6–85 days.

2.2 Mass spectrometry

2.2.1 This study

Sample Δ_{47} was measured from January 2018 to November 2020 at the MIT Carbonate Research Laboratory on a Nu Perspective dual-inlet isotope ratio mass spectrometer with a NuCarb automated sample preparation unit held at 70°C (see Mackey et al., 2020). Carbonate samples (including dolomite) weighing 400–600 µg reacted for 25 minutes in individual glass vials with 150 µl orthophosphoric acid ($\varrho = 1.93$ g/cm^3). Evolved CO_2 gas was purified cryogenically and by passive passage through a Porapak trap (1/4" ID; 0.4 g 50/80 mesh Porapak Q) held at -30°C. Purified sample gas and reference gas

Table 1. Description of analyzed and reanalyzed samples.

Study	Mineralogy	Formation	Formation Temp. Range (°C)[a]	Samples Analyzed (this study; orig. study)
Bonifacie et al. (2017)	Dolo., proto-dolo.	Mixed solution	80–350	4; 17
Kele et al. (2015)	Calc. (minor arag.)	Tufa, travertine	5–95	12; 24
Kelson et al. (2017)	Calc. (minor arag.)	Active/passive degas, mixed sol'n	6–78	15; 56
Kluge et al. (2015)	Calc., arag.	Active degas	25–80	2; 29
This study	Calc.	Lacustrine, experimentally heated	0.5–1100	8

[a]Temperature range is only for samples reanalyzed in this study.

of known composition were alternately measured on six Faraday collectors (m/z 44–49) in 3 acquisitions of 20 cycles, each with 30 second integration time (30 minute total integration time). Initial voltage was 8–20 V on the m/z 44 beam with 2×10^8 Ω resistors and depleted by approximately 50% over the course of an analysis. Sample and standard gases depleted at equivalent rates from microvolumes over the integration time.

Each run of approximately 50 individual analyses began with each of ETH-1–ETH-4 in random order, and then alternated between blocks of three unknowns and two ETH anchors. Additionally, IAEA-C1, IAEA-C2, and MERCK were respectively measured once per run. Unknown to anchor ratio was planned at 1:1 for each run, although gas preparation or mass spectrometer error occasionally modified this ratio. The reference side of the dual-inlet was refilled with reference gas every 10 to 17 analyses. In total, unknowns were measured 6–16 times over the study interval (362 total unknown analyses).

2.3 Data processing

Raw mass spectrometer data were first processed by removing cycles (i.e., single integration cycles) with raw Δ_{47} values more than 5 "long-term" standard deviations (the mean of the respective cycle-level SD for ETH-1–4 over a 3-month period, 0.10‰) away from the median Δ_{47} measurement for the analysis. Analyses with more than 20 cycles (out of 60 total cycles) falling outside the 5 long-term SD threshold were removed.

199 In total, 0.81% of cycles and 0.42% of analyses were removed. No pressure baseline cor-

200 rection was applied. Long-term repeatability (1SD) of Δ_{47} for all analyses (after data

201 processing described above) is 0.036 ‰.

202 After cycle-level outlier removal, data were processed using the 'D47crunch' Python

203 package (Daëron, submitted) using IUPAC ^{17}O parameters, 70°C ^{18}O acid fractionation

204 factor of 1.00871 (Kim et al., 2007), and projected to the I-CDES with values for ETH-

205 1–4, IAEA-C2, and MERCK from the InterCarb exercise (Bernasconi et al., submitted),

206 which uses nominal Δ_{47} values for the carbonates determined at an acid reaction tem-

207 perature of 90°C (0.088‰ lower than values determined at 25°C) after Petersen et al.

208 (2019). Raw Δ_{47} measurements were converted to the I-CDES using a pooled regres-

209 sion approach that accounts for the relative mapping of all samples in δ^{47}-Δ_{47} space (Daëron,

210 submitted). Analytical uncertainty and error associated with creation of the reference

211 frame were fully propagated through the dataset. A full description of the data reduc-

212 tion procedure used in D47crunch is detailed in (Daëron, submitted). Each run (typi-

213 cally 50 analyses) was treated as an analytical session. IAEA-C1 was treated as an un-

214 known and used as an internal consistency check (n = 16, mean = 0.292‰, 1SE = 0.098‰).

215 Finally, Peirce's criterion (Ross, 2003; Zaarur et al., 2013) was applied to the dataset at

216 the analysis level; a total of six analyses were marked as outliers and removed, followed

217 by reprocessing of the dataset.

3 Results and Discussion

219 Results for all analyses (re)analyzed here are summarized at the sample level in Ta-

220 ble 2 (see Dataset S1 and S2 for full results). Accounting for uncertainty in Δ_{47} (long-

221 term repeatability, 1SD) and formation temperature (0.5–10°C) with the regression method

222 described in York et al. (2004), these data define a linear $1/T^2$-Δ_{47} relationship from 0.5°C–

223 1100°C shown in Figure 1.

3.1 Comparison of T-Δ_{47} relationship across sample types

225 After applying the 90°C acid fractionation factor of 0.088 ‰(Petersen et al., 2019),

226 the published regression equations from Kele et al. (2015); Kluge et al. (2015); Kelson

227 et al. (2017); Bonifacie et al. (2017) all fall within the 95% confidence interval of the re-

228 gressions defined by this study's reanalysis of their constituent samples (supporting in-

229   formation Fig. S3). Natural and lab-precipitated samples fall on nearly identical regres-

230   sion lines (Fig. 2A); analysis of covariance (ANCOVA) fails to reject the null hypoth-

231   esis that both types of samples are characterized by a single regression line at the 95%

232   confidence level at our typical sample precision levels (1SE) of ∼10 ppm ($p_{slope} = 0.43$,

233   $p_{intercept} = 0.17$; see Table S1 in supporting information for full table of ANCOVA anal-

234   yses). Natural samples display a weaker correlation coefficient ($r^2 = 0.96$ vs. 0.99) and

235   larger error of the estimate, likely due to the greater variability of fluid temperature in

236   natural settings.

237   Our reanalysis of samples precipitated by Kelson et al. (2017) supports their con-

238   clusions: we observe no statistically significant Δ_{47} offset between passively and actively

239   degassed samples ($p_{slope} = 0.19$, $p_{intercept} = 0.79$) or with the addition of carbonic an-

240   hydrase ($p_{slope} = 0.79$, $p_{intercept} = 0.32$; Fig. S1). Reanalysis of samples from Kele et

241   al. (2015) and Kelson et al. (2017) confirms the conclusions of Kele et al. (2015) that there

242   is no significant difference between samples precipitated at low ($<$ 7) vs. high ($>$ 7)

243   pH ($p_{slope} = 0.4$, $p_{intercept} = 0.99$) or intensive vs. moderate precipitation rate (p_{slope}

244   $= 0.05$, $p_{intercept} = 0.11$; Fig. S2). The low number of rapid precipitates (particularly

245   at low temperatures) makes the above claim inconclusive, but Δ_{47} values for two extremely

246   slow-growing samples re-analyzed for this study at LCSE on an Isoprime 100 mass spec-

247   trometer (see Text S3), respectively from Devil's Hole, NV, USA, and Laghetto Basso,

248   Italy (see Winograd et al., 2006; Coplen, 2007; Drysdale et al., 2012; Daëron et al., 2019),

249   are within 0.001‰of the expected values based on the calibration from this study (Fig.

250   3B). Calcite-water fractionation in ^{18}O calculated from a subset of 20 samples with fluid

251   δ^{18}O data (Fig. S5) agrees closely with the equations of Coplen (2007) and Daëron et

252   al. (2019). The Antarctic microbially-mediated lacustrine calcites show no discernible

253   offset from the overall trend, but small sample numbers and limited temperature range

254   prohibit formal analysis.

255   With only three stoichiometric dolomite samples, no stoichiometric dolomite sam-

256   ples below 100°C, and no calcite samples between 95°C and 1100°C measured for this

257   study, we cannot rigorously compare calcite and dolomite regressions; ANCOVA vari-

258   ably accepts/rejects the null hypothesis depending on categorization of the single protodolomite

259   sample. Therefore, we cannot assert that dolomite and calcite samples can be described

260   using a single regression equation, as previously suggested by Bonifacie et al. (2017) and

261   Petersen et al. (2019); analysis of dolomite samples with lower ($<$ 80°C) and higher ($>$

–9–

262 350°C) formation temperature is needed. The regression through aragonite-containing

263 samples (four samples < 6%; one sample = 38%; one sample = 78%) is statistically sim-

264 ilar to the regression through all calcite samples (Fig. 2B). A single sample (Aqua Borra)

265 with minor goethite (15%) has individual Δ_{47} analyses both much higher and lower than

266 expected, but has a mean Δ_{47} value that closely agrees with the regression presented here.

267 The absence of systematic offset in the T-Δ_{47} relationship corresponding to any

268 known sample characteristic suggests that discrepancies between these exact samples from

269 previous calibration efforts are not a function of the character of measured sample ma-

270 terial (Wacker et al., 2014; Kele et al., 2015; Kluge et al., 2015; Kelson et al., 2017; Boni-

271 facie et al., 2017). Furthermore, the consistency of the T-Δ_{47} relationship across a broad

272 range of materials and temperatures (e.g., from Antarctic lacustrine microbially-mediated

273 carbonates to laboratory-grown carbonates heated to 1100°C) indicates that a single T-

274 Δ_{47} calibration can adequately describe a wide variety of sample types.

3.2 Comparison across calibration studies using carbonate-based standardization

277 Reprocessing data from recent calibration studies (Breitenbach et al., 2018; Peral

278 et al., 2018; Meinicke et al., 2020; Jautzy et al., 2020) with updated InterCarb anchor

279 values (Bernasconi et al., submitted) yields an almost identical regression to that cal-

280 culated in this study (Fig. 3). The near-perfect agreement of these calibrations ($\sim$0.2°C

281 offset near 25°C and 100°C) despite differences in sample material and measurement method

282 points to the strength of carbonate-based standardization and the potential of a unified

283 clumped isotope calibration.

284 The clumped isotope calibration reported here covers the broadest range of tem-

285 peratures, includes diverse carbonates, replicates measurements several times, and uses

286 a low unknown:anchor ratio to firmly tie unknown measurements to the I-CDES. How-

287 ever, this calibration has an unequal distribution of samples in $1/T^2$ space, is anchored

288 at the coldest temperatures by unusual carbonates, and does not contain marine carbon-

289 ates, which are of particular interest to the clumped isotope community. To address these

290 weaknesses, we combine data from this study with four other carbonate-standardized cal-

291 ibrations (Peral et al., 2018; Meinicke et al., 2020; Jautzy et al., 2020, only cave sam-

292 ples from Breitenbach et al., 2018) to present a composite $1/T^2$-Δ_{47} regression that has

smaller temperature gaps, is anchored at low temperatures by a variety of samples, and

extends the calibration to biogenic marine carbonates:

$$\Delta_{47(I-CDES90°C)} = 0.0390 \pm 0.0004 \times \frac{10^6}{T^2} + 0.154 \pm 0.004 \ (r^2 = 0.97) \tag{1}$$

Along with excellent agreement between laboratories using carbonate-based standardization, this dataset and the community-developed InterCarb anchor values (Bernasconi et al., submitted) narrow the discrepancy between calibrations using carbonate anchor values and heated/equilibrated gases, most notably Petersen et al. (2019). Specifically, calibrations of Jautzy et al. (2020) and Petersen et al. (2019) differed by 5°C near 25°C and 20°C near 100°C; the composite calibration regression shown in Equation 1 differs from Petersen et al. (2019) by 3°C near 25°C and by 7°C near 100°C (Fig. 1A).

3.3 Non-linearity of $1/T^2$-Δ_{47} relationship for high-temperature precipitates

At high temperatures, theory predicts a non-linear $1/T^2$-Δ_{47} relationship (e.g., Guo et al., 2009; Hill et al., 2014), supported by recent empirical calibrations (e.g., Müller et al., 2019; Jautzy et al., 2020). A third-order polynomial regression through our data falls within the 95% CL of our linear fit over the entire temperature range (Fig. 3A) and does not improve the goodness of fit ($r^2 = 0.97$ for both); we observe no evidence that a non-linear fit better describes high-temperature data.

4 Conclusions

When measured in a consistent analytical setting with carbonate-based standardization, no systematic offset is observed between samples precipitated across a broad spectrum of conditions that were previously determined to have disparate Δ_{47} values. Among sample types measured here, we find no evidence that the particular character of sample material (e.g., mineralogy, addition of carbonic anhydrase, pH, precipitation rate, biological mediation) influences the Δ_{47} calibration, although calcite and dolomite agreement remain inconclusive.

Furthermore, when anchor values from the InterCarb exercise (Bernasconi et al., submitted) are used with data reduction best practices (Petersen et al., 2019; Daëron,

Table 2. Final corrected $\delta^{13}C_{VPDB}$ (‰), $\delta^{18}O_{VSMOW}$ (‰), and $\Delta_{47(CDES90°C)}$ (‰) results.

Sample name	Author	Mineralogy	Method	T(°C)	N	$\delta^{13}C$	$\delta^{18}O$	Δ_{47}	SE	95% CL
IPGP_100-A3	Bonifacie	Dolomite	Lab	102.3	9	-46.3	-17.4	0.427	0.015	0.029
IPGP_250-A5	Bonifacie	Dolomite	Lab	252.1	9	-52.8	-28.0	0.275	0.025	0.049
IPGP_350-A9	Bonifacie	Dolomite	Lab	351.4	10	-55.6	-32.0	0.232	0.018	0.035
IPGP_80-1	Bonifacie	Proto-dolo.	Lab	80.2	10	-6.9	-16.2	0.495	0.012	0.024
ETH-1-1100-SAM	This study	Calcite	Lab	1100	10	2.0	-2.0	0.178	0.018	0.036
ETH-2-1100-SAM	This study	Calcite	Lab	1100	10	-10.1	-18.4	0.192	0.017	0.034
HT_25C	Kluge	Calcite	Lab	25	9	2.1	-6.2	0.610	0.013	0.026
HT_80C	Kluge	Aragonite	Lab	80	9	1.1	-15.4	0.487	0.013	0.025
AQUA_BORRA	Kele	Calcite	Natural	36.1	11	1.7	-8.4	0.577	0.012	0.023
BUK_4	Kele	Calcite	Natural	54.9	9	2.2	-15.0	0.541	0.013	0.025
CANARIAN	Kele	Calcite	Natural	33.8	8	0.1	-10.2	0.584	0.014	0.027
CANNATOPA	Kele	Calcite	Natural	11	8	-4.1	-5.4	0.628	0.014	0.027
IGAL	Kele	Calcite	Natural	75	10	0.6	-13.5	0.475	0.012	0.024
LAPIGNA	Kele	Calcite	Natural	12.5	9	-11.4	-5.5	0.621	0.013	0.026
NG_2	Kele	Calcite	Natural	60.4	9	3.6	-24.6	0.505	0.013	0.025
P5_SUMMER	Kele	Calcite	Natural	12	9	5.4	-14.3	0.633	0.013	0.026
P5_WINTER	Kele	Calcite	Natural	5	10	5.1	-12.7	0.635	0.013	0.026
SARTEANO	Kele	Calcite	Natural	20.7	9	0.4	-7.3	0.594	0.013	0.025
SZAL-2	Kele	Calcite	Natural	11	9	-10.3	-8.2	0.654	0.013	0.026
TURA	Kele	Calcite	Natural	95	9	3.7	-23.2	0.409	0.013	0.025
LF2012-9_7-A	This study	Calcite	Natural	2.5	4	2.6	-27.2	0.663	0.023	0.045
LF2012-D1-A	This study	Calcite	Natural	2.5	4	3.4	-27.1	0.658	0.023	0.044
LJ2010-12A-Z1A	This study	Calcite	Natural	0.5	13	7.7	-39.4	0.668	0.014	0.028
LJ2010-12A-Z2A	This study	Calcite	Natural	0.5	6	8.1	-38.1	0.672	0.020	0.039
LJ2010-5B-A	This study	Calcite	Natural	0.5	11	8.1	-37.6	0.676	0.014	0.027
LV26NOV10-2A	This study	Calcite	Natural	4	6	11.2	-29.0	0.652	0.018	0.035
UWCP14_20C_9	Kelson	Calcite	Lab	23	8	-21.1	-10.8	0.604	0.014	0.028
UWCP14_20C_CA_11	Kelson	Calcite	Lab	23	10	-14.1	-10.9	0.615	0.013	0.025
UWCP14_21C_1	Kelson	Calcite	Lab	22	8	-18.6	-11.1	0.611	0.014	0.028
UWCP14_4C_3	Kelson	Calcite	Lab	6	8	-21.3	-6.6	0.650	0.014	0.028
UWCP14_4C_4	Kelson	Calcite	Lab	6	9	-23.4	-6.7	0.658	0.013	0.026
UWCP14_50C_2	Kelson	Calcite	Lab	51	9	-18.4	-16.4	0.534	0.013	0.026
UWCP14_50C_7	Kelson	Calcite	Lab	54	9	-0.2	-17.4	0.518	0.013	0.025
UWCP14_50C_CA_11	Kelson	Calcite	Lab	50	9	-18.5	-15.9	0.527	0.014	0.027
UWCP14_60C_2	Kelson	Calcite	Lab	66	9	-12.5	-18.2	0.491	0.013	0.026
UWCP14_70C_4	Kelson	Calcite	Lab	72	8	-17.7	-18.8	0.490	0.014	0.028
UWCP14_70C_CA_4	Kelson	Calcite	Lab	71	9	-0.2	-19.6	0.493	0.013	0.025
UWCP14_80C_2	Kelson	Calcite	Lab	78	9	-6.9	-20.9	0.483	0.013	0.025
UWCP14_8C_2	Kelson	Calcite	Lab	9	9	-15.1	-7.7	0.633	0.013	0.026
UWCP14_8C_6	Kelson	Calcite	Lab	9	9	0.4	-8.8	0.648	0.013	0.026
UWCP14_8C_CA_4	Kelson	Calcite	Lab	9	8	-17.4	-8.1	0.648	0.014	0.028

submitted), the $1/T^2$-Δ_{47} regression defined by data presented here is nearly identical (0.2°C offset at 25°C and 100°C) to the regression defined by a suite of recent calibration studies (Peral et al., 2018; Breitenbach et al., 2018; Meinicke et al., 2020; Jautzy et al., 2020) and closely approximates the composite calibration of Petersen et al. (2019). Equation 1 spans the broadest range of temperatures measured in a consistent analytical setting and, when corrected with carbonate anchor values from the InterCarb exercise (Bernasconi et al., submitted) or heated/equilibrated gases, may be applied across a wide range of natural and laboratory-grown carbonate material.

References

Bernasconi, S. M., Daëron, M., Bergmann, K. D., Bonifacie, M., Meckler, A. N., Affek, H. P., ... Ziegler, M. (submitted). InterCarb: A community effort to improve inter-laboratory standardization of the carbonate clumped isotope thermometer using carbonate standards. *Geochemistry, Geophysics, Geosystems*. doi: 10.1002/essoar.10504430.4

Bernasconi, S. M., Müller, I. A., Bergmann, K. D., Breitenbach, S. F., Fernandez, A., Hodell, D. A., ... Ziegler, M. (2018). Reducing uncertainties in carbonate clumped isotope analysis through consistent carbonate-based standardization. *Geochemistry, Geophysics, Geosystems*, *19*(9), 2895–2914. doi: 10.1029/2017GC007385

351 Bonifacie, M., Calmels, D., Eiler, J. M., Horita, J., Chaduteau, C., Vasconcelos, C.,
352 ... Bourrand, J. J. (2017). Calibration of the dolomite clumped isotope ther-
353 mometer from 25 to 350 C, and implications for a universal calibration for all
354 (Ca, Mg, Fe)CO3carbonates. *Geochimica et Cosmochimica Acta*, *200*, 255–279.
355 doi: 10.1016/j.gca.2016.11.028

356 Brand, W. A., Assonov, S. S., & Coplen, T. B. (2010). Correction for the 17O
357 interference in δ13C measurements when analyzing CO2 with stable isotope
358 mass spectrometry (IUPAC Technical Report). *Pure Applied Chemistry*, *82*(8),
359 1719–1733. doi: 10.1351/PAC-REP-09-01-05

360 Breitenbach, S. F., Mleneck-Vautravers, M. J., Grauel, A. L., Lo, L., Bernasconi,
361 S. M., Müller, I. A., ... Hodell, D. A. (2018). Coupled Mg/Ca and
362 clumped isotope analyses of foraminifera provide consistent water temper-
363 atures. *Geochimica et Cosmochimica Acta*, *236*, 283–296. doi: 10.1016/
364 j.gca.2018.03.010

365 Coplen, T. B. (2007). Calibration of the calcite-water oxygen-isotope geothermome-
366 ter at Devils Hole, Nevada, a natural laboratory. *Geochimica et Cosmochimica
367 Acta*, *71*(16), 3948–3957. doi: 10.1016/j.gca.2007.05.028

368 Daëron, M. (submitted). Full propagation of analytical uncertainties in D47
369 measurements. *Geochemistry, Geophysics, Geosystems*. doi: 10.1002/
370 essoar.10504430.4

371 Daëron, M., Blamart, D., Peral, M., & Affek, H. P. (2016). Absolute isotopic abun-
372 dance ratios and the accuracy of Δ47measurements. *Chemical Geology*, *442*,
373 83–96. doi: 10.1016/j.chemgeo.2016.08.014

374 Daëron, M., Drysdale, R. N., Peral, M., Huyghe, D., Blamart, D., Coplen,
375 T. B., ... Zanchetta, G. (2019). Most Earth-surface calcites precipitate
376 out of isotopic equilibrium. *Nature Communications*, *10*(1), 1–7. doi:
377 10.1038/s41467-019-08336-5

378 Dennis, K. J., Affek, H. P., Passey, B. H., Schrag, D. P., & Eiler, J. M. (2011).
379 Defining an absolute reference frame for clumped' isotope studies of
380 CO2. *Geochimica et Cosmochimica Acta*, *75*(22), 7117–7131. Retrieved
381 from http://dx.doi.org/10.1016/j.gca.2011.09.025 doi: 10.1016/
382 j.gca.2011.09.025

383 Dennis, K. J., & Schrag, D. P. (2010). Clumped isotope thermometry of carbon-

atites as an indicator of diagenetic alteration. *Geochimica et Cosmochimica Acta*, *74*(14), 4110–4122. doi: 10.1016/j.gca.2010.04.005

Drysdale, R. N., Paul, B. T., Hellstrom, J. C., Couchoud, I., Greig, A., Bajo, P., ... Woodhead, J. D. (2012). Precise microsampling of poorly laminated speleothems for U-series dating. *Quaternary Geochronology*, *14*, 38–47. doi: 10.1016/j.quageo.2012.06.009

Finnegan, S., Bergmann, K., Eiler, J. M., Jones, D. S., Fike, D. A., Eisenman, I., ... Fischer, W. W. (2011). The magnitude and duration of Late Ordovician-Early Silurian glaciation. *Science*, *331*(6019), 903–906. doi: 10.1126/science.1200803

Ghosh, P., Adkins, J., Affek, H., Balta, B., Guo, W., Schauble, E. A., ... Eiler, J. M. (2006). 13C-18O bonds in carbonate minerals: A new kind of pale-othermometer. *Geochimica et Cosmochimica Acta*, *70*(6), 1439–1456. doi: 10.1016/j.gca.2005.11.014

Guo, W., Mosenfelder, J. L., Goddard, W. A., & Eiler, J. M. (2009). Isotopic fractionations associated with phosphoric acid digestion of carbonate minerals: Insights from first-principles theoretical modeling and clumped isotope measurements. *Geochimica et Cosmochimica Acta*, *73*(24), 7203–7225. doi: 10.1016/j.gca.2009.05.071

Hill, P. S., Tripati, A. K., & Schauble, E. A. (2014). Theoretical constraints on the effects of pH, salinity, and temperature on clumped isotope signatures of dissolved inorganic carbon species and precipitating carbonate minerals. *Geochimica et Cosmochimica Acta*, *125*, 610–652. doi: 10.1016/j.gca.2013.06.018

Horita, J. (2014). Oxygen and carbon isotope fractionation in the system dolomite-water-CO2 to elevated temperatures. *Geochimica et Cosmochimica Acta*, *129*, 111–124. doi: 10.1016/j.gca.2013.12.027

Huntington, K. W., Eiler, J. M., Affek, H. P., Guo, W., Bonifacie, M., Yeung, L. Y., ... Came, R. (2009). Methods and limitations of 'clumped' CO2 isotope (Δ47) analysis by gas-source isotope ratiomass spectrometry. *Journal of Mass Spectrometry*, *44*(9), 1318–1329. doi: 10.1002/jms.1614

Jautzy, J., Savard, M., Dhillon, R., Bernasconi, S., Lavoie, D., & Smirnoff, A. (2020). Clumped isotope temperature calibration for calcite: Bridging the-

ory and experimentation. *Geochemical Perspective Letters*, *14*, 36–41. doi: 10.7185/geochemlet.2021

Jungblut, A. D., Hawes, I., Mackey, T. J., Krusor, M., Doran, P. T., Sumner, D. Y., ... Goroncy, A. K. (2016). Microbial mat communities along an oxygen gradient in a perennially ice-covered Antarctic lake. *Applied and Environmental Microbiology*, *82*(2), 620–630. doi: 10.1128/AEM.02699-15

Kele, S., Breitenbach, S. F., Capezzuoli, E., Meckler, A. N., Ziegler, M., Millan, I. M., ... Bernasconi, S. M. (2015). Temperature dependence of oxygen- and clumped isotope fractionation in carbonates: A study of travertines and tufas in the 6-95C temperature range. *Geochimica et Cosmochimica Acta*, *168*, 172–192. doi: 10.1016/j.gca.2015.06.032

Kelson, J. R., Huntington, K. W., Schauer, A. J., Saenger, C., & Lechler, A. R. (2017). Toward a universal carbonate clumped isotope calibration: Diverse synthesis and preparatory methods suggest a single temperature relationship. *Geochimica et Cosmochimica Acta*, *197*, 104–131. doi: 10.1016/j.gca.2016.10.010

Kim, S. T., Mucci, A., & Taylor, B. E. (2007). Phosphoric acid fractionation factors for calcite and aragonite between 25 and 75C: Revisited. *Chemical Geology*, *246*(3-4), 135–146. doi: 10.1016/j.chemgeo.2007.08.005

Kluge, T., John, C. M., Jourdan, A. L., Davis, S., & Crawshaw, J. (2015). Laboratory calibration of the calcium carbonate clumped isotope thermometer in the 25-250C temperature range. *Geochimica et Cosmochimica Acta*, *157*, 213–227. doi: 10.1016/j.gca.2015.02.028

Lloyd, M. K., Eiler, J. M., & Nabelek, P. I. (2017). Clumped isotope thermometry of calcite and dolomite in a contact metamorphic environment. *Geochimica et Cosmochimica Acta*, *197*, 323–344. doi: 10.1016/j.gca.2016.10.037

Mackey, T. J., Jost, A. B., Creveling, J. R., & Bergmann, K. D. (2020). A Decrease to Low Carbonate Clumped Isotope Temperatures in Cryogenian Strata. *AGU Advances*, *1*(3). doi: 10.1029/2019av000159

Mackey, T. J., Sumner, D. Y., Hawes, I., & Jungblut, A. D. (2017). Morphological signatures of microbial activity across sediment and light microenvironments of Lake Vanda, Antarctica. *Sedimentary Geology*, *361*, 82–92. doi: 10.1016/j.sedgeo.2017.09.013

–16–

Mackey, T. J., Sumner, D. Y., Hawes, I., Leidman, S. Z., Andersen, D. T., & Jung-blut, A. D. (2018). Stromatolite records of environmental change in perennially ice-covered Lake Joyce, McMurdo Dry Valleys, Antarctica. *Biogeochemistry*, *137*(1-2), 73–92. doi: 10.1007/s10533-017-0402-1

Mangenot, X., Gasparrini, M., Gerdes, A., Bonifacie, M., & Rouchon, V. (2018). An emerging thermochronometer for carbonate-bearing rocks: Δ47 /(U-Pb). *Geology*, *46*(12), 1067–1070. doi: 10.1130/G45196.1

Meinicke, N., Ho, S. L., Hannisdal, B., Nürnberg, D., Tripati, A., Schiebel, R., & Meckler, A. N. (2020). A robust calibration of the clumped isotopes to temperature relationship for foraminifers. *Geochimica et Cosmochimica Acta*, *270*, 160–183. doi: 10.1016/j.gca.2019.11.022

Müller, I. A., Rodriguez-Blanco, J. D., Storck, J.-C., Santilli, G., Bontognali, T. R. R., Vasconcelos, C., ... Bernasconi, S. M. (2019). Calibration of the oxygen and clumped isotope thermometers for (proto-) dolomite based on synthetic and natural carbonates. *Chemical Geology*, *525*, 1–17. doi: 10.1016/j.chemgeo.2019.07.014

Peral, M., Daëron, M., Blamart, D., Bassinot, F., Dewilde, F., Smialkowski, N., ... Waelbroeck, C. (2018). Updated calibration of the clumped isotope thermometer in planktonic and benthic foraminifera. *Geochimica et Cosmochimica Acta*, *239*, 1–16. doi: 10.1016/j.gca.2018.07.016

Petersen, S. V., Defliese, W. F., Saenger, C., Daëron, M., Huntington, K. W., John, C. M., ... Winkelstern, I. Z. (2019). Effects of improved 17O correction on interlaboratory agreement in clumped isotope calibrations, estimates of mineralspecific offsets, and temperature dependence of acid digestion fractionation. *Geochemistry, Geophysics, Geosystems*, 3495–3519. doi: 10.1029/2018gc008127

Piasecki, A., Bernasconi, S. M., Grauel, A. L., Hannisdal, B., Ho, S. L., Leutert, T. J., ... Meckler, N. (2019). Application of clumped isotope thermometry to benthic foraminifera. *Geochemistry, Geophysics, Geosystems*, *20*(4), 2082–2090. doi: 10.1029/2018GC007961

Ross, S. (2003). Peirce's criterion for the elimination of suspect experimental data. *Journal of Engineering Technology*, *20*, 1–12.

Schauble, E. A., Ghosh, P., & Eiler, J. M. (2006). Preferential formation of

13C 18O bonds in carbonate minerals, estimated using first-principles lattice dynamics. *Geochimica et Cosmochimica Acta*, *70*(10), 2510–2529. doi: 10.1016/j.gca.2006.02.011

Schauer, A. J., Kelson, J., Saenger, C., & Huntington, K. W. (2016). Choice of 17O correction affects clumped isotope ($\Delta 47$) values of CO2 measured with mass spectrometry. *Rapid Communications in Mass Spectrometry*, *30*(24), 2607–2616. doi: 10.1002/rcm.7743

Snell, K. E., Thrasher, B. L., Eiler, J. M., Koch, P. L., Sloan, L. C., & Tabor, N. J. (2013). Hot summers in the Bighorn Basin during the early Paleogene. *Geology*, *41*(1), 55–58. doi: 10.1130/G33567.1

Wacker, U., Fiebig, J., Tödter, J., Schöne, B. R., Bahr, A., Friedrich, O., . . . Joachimski, M. M. (2014). Empirical calibration of the clumped isotope paleothermometer using calcites of various origins. *Geochimica et Cosmochimica Acta*, *141*, 127–144. Retrieved from `10.1016/j.gca.2014.06.004`

Winkelstern, I. Z., & Lohmann, K. C. (2016). Shallow burial alteration of dolomite and limestone clumped isotope geochemistry. *Geology*, *44*(6), 467–470. doi: 10 .1130/G37809.1

Winograd, I. J., Landwehr, J. M., Coplen, T. B., Sharp, W. D., Riggs, A. C., Ludwig, K. R., & Kolesar, P. T. (2006). Devils Hole, Nevada, $\delta 18O$ record extended to the mid-Holocene. *Quaternary Research*, *66*(2), 202–212. doi: 10.1016/j.yqres.2006.06.003

York, D., Evensen, N. M., López, M., & Delgado, J. D. B. (2004). Unified equations for the slope, intercept, and standard errors of the best straight line. *American Journal of Physics*, *72*(3), 367–373. doi: 10.1119/1.1632486

Zaarur, S., Affek, H. P., & Brandon, M. T. (2013). A revised calibration of the clumped isotope thermometer. *Earth and Planetary Science Letters*, *382*, 47–57. Retrieved from `http://dx.doi.org/10.1016/j.epsl.2013.07.026` doi: 10.1016/j.epsl.2013.07.026
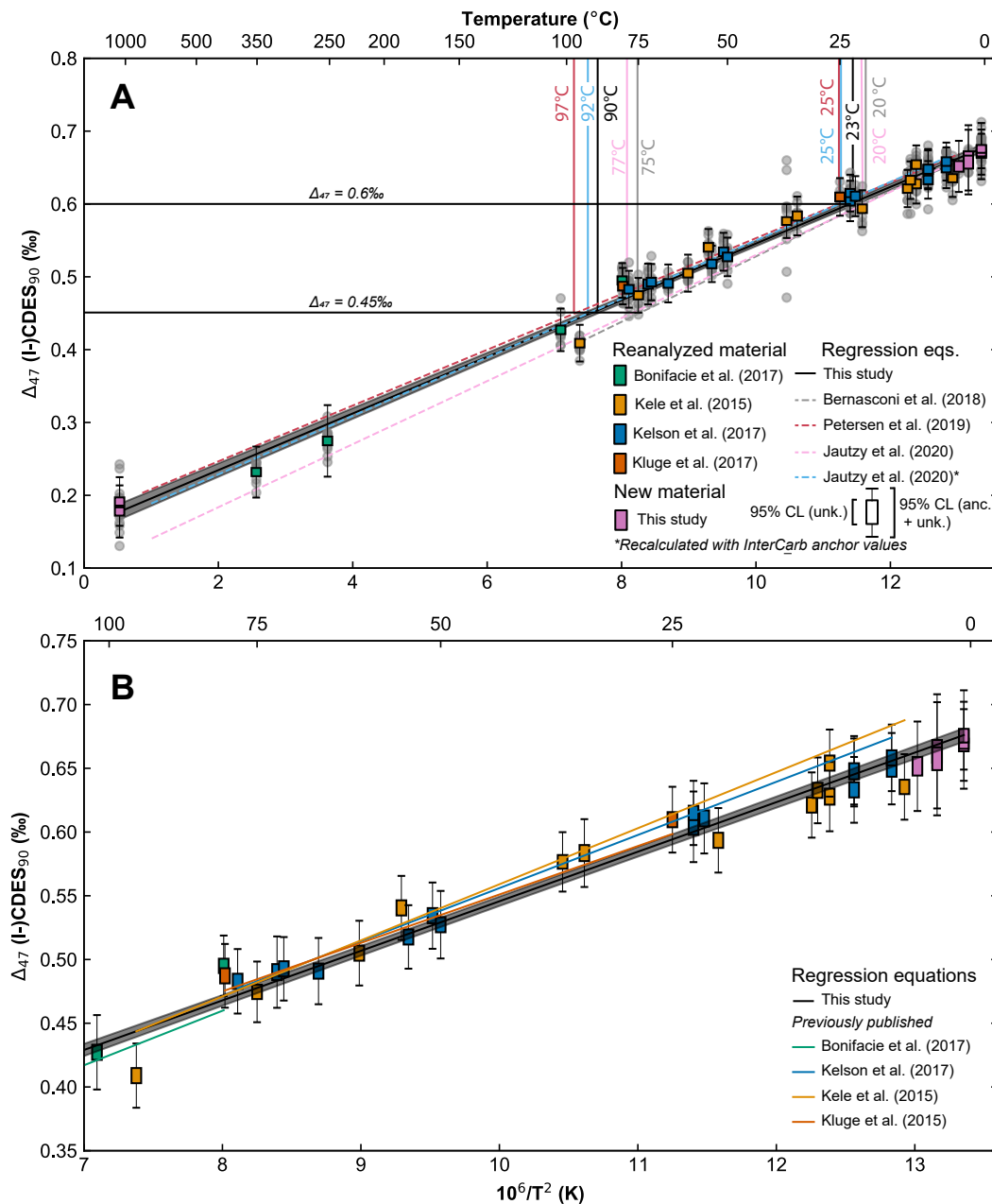
Figure 1. A. Linear $1/T^2$-Δ_{47} regression and 95% confidence interval (York et al., 2004) for samples (re)analyzed in this study shown with recently published calibrations. Solid vertical lines show approximate formation temperature for each calibration when $\Delta_{47} = 0.45‰$ and $\Delta_{47} = 0.6‰$. Error bars correspond to 95% confidence limits accounting for error from unknown and anchor analyses; boxes correspond to 95% CL not accounting for normalization errors; gray circles show individual analyses. The regression from this study is nearly identical to the regression from Jautzy et al. (2020) when all Δ_{47} values are calculated with 'InterCarb' (Bernasconi et al., submitted) anchor values. B. T-Δ_{47} relationship for samples 0–100°C including regressions from studies with material reanalyzed for this study (Bonifacie et al. (2017), Eq. 1; Kele et al. (2015), Eq. 1; Kelson et al. (2017) Eq. 1; Kluge et al. (2015), Table 1, 'This study, linear fit'; all converted to 90°C acid temperature using AFF values from Petersen et al., 2019).
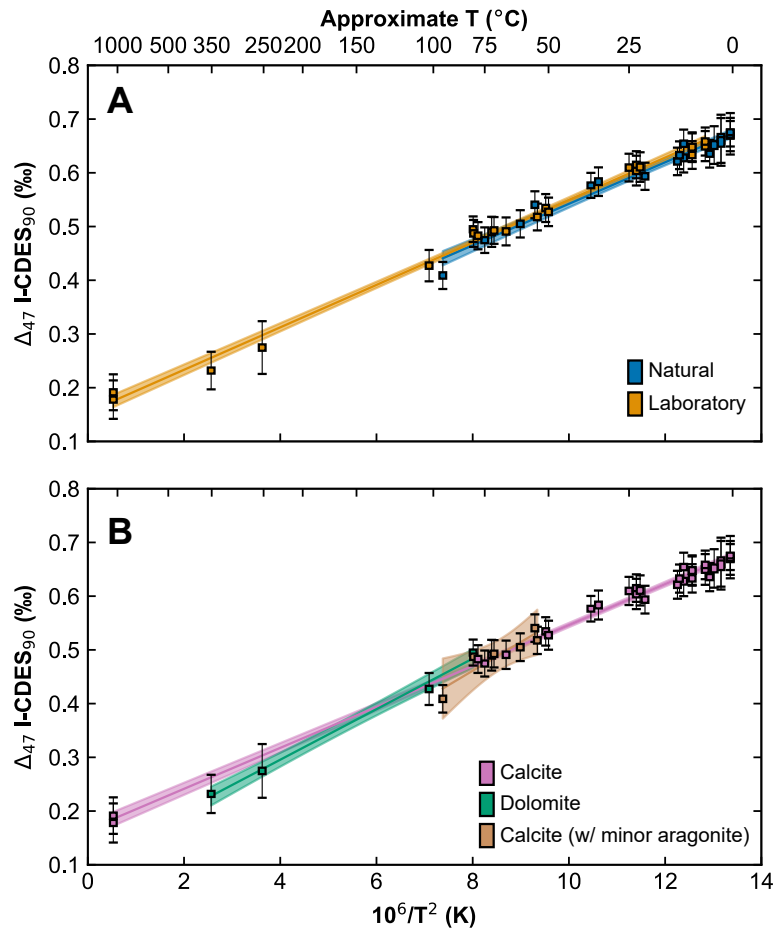
-19-

Figure 2. A. $1/T^2$-Δ_{47} comparison of natural and laboratory precipitated sample material. Error bars correspond to 95% confidence limits accounting for error from both unknown and anchor analyses; boxes correspond to 95% CL not accounting for normalization errors. Natural samples have larger uncertainty of the estimate and a poorer fit, likely due to natural variability in formation temperature and a smaller temperature range. B. Comparison of calcite, (proto)dolomite, and aragonite sample material. The regression lines between calcite and dolomite diverge but 95% confidence intervals overlap; divergence of regression equations may be related to the small temperature range of dolomite (relative to calcite) measured in this study and the small number of dolomite samples.
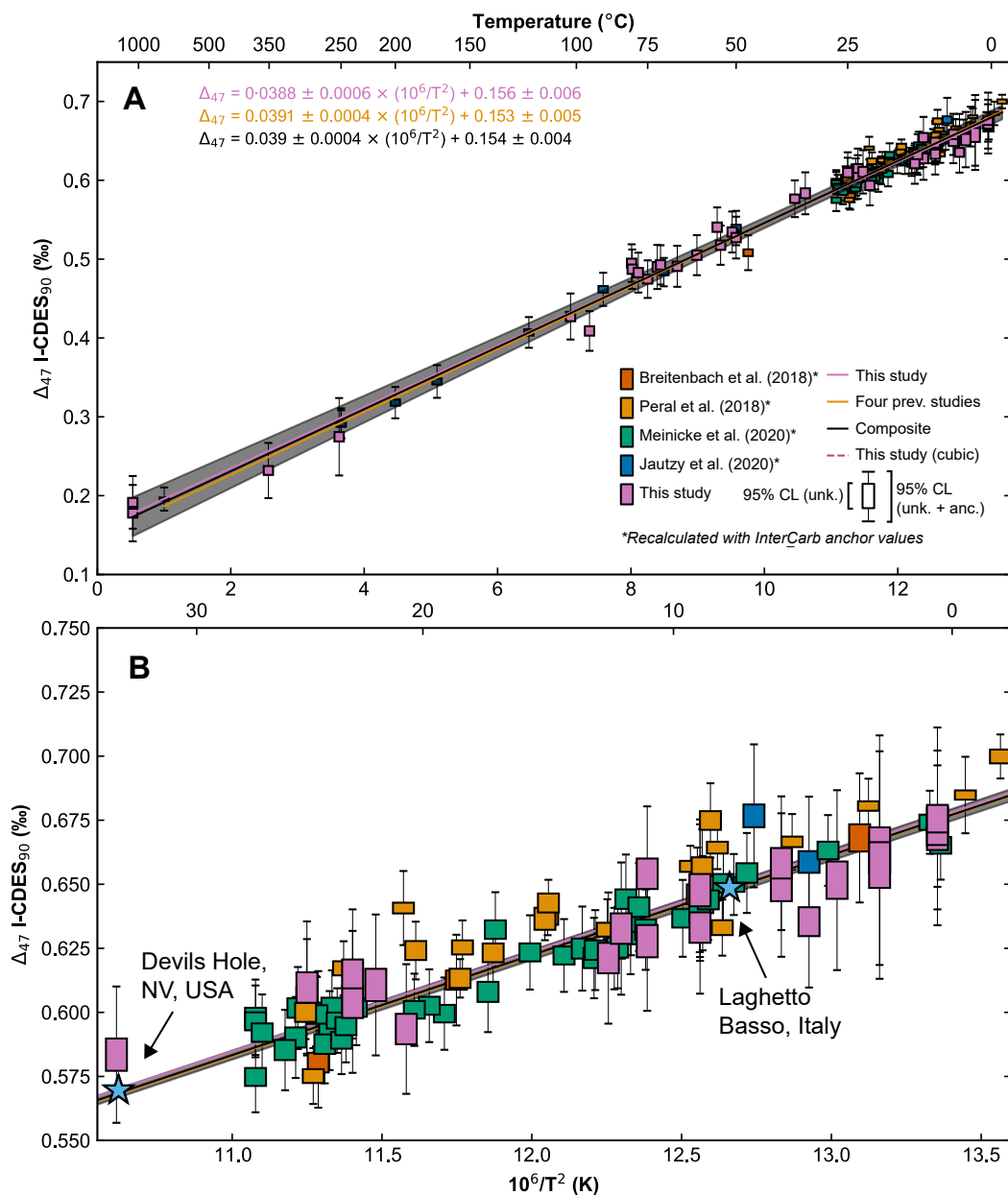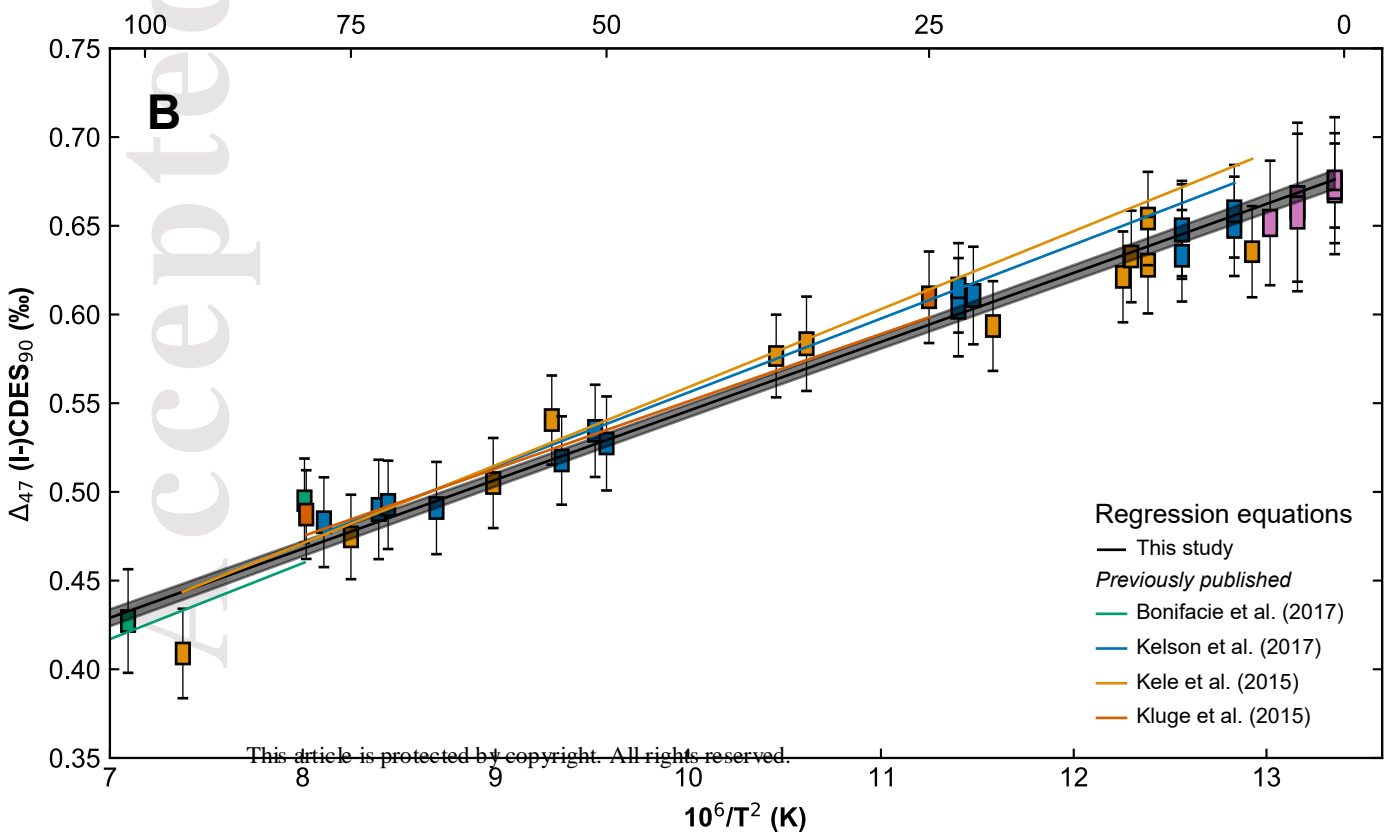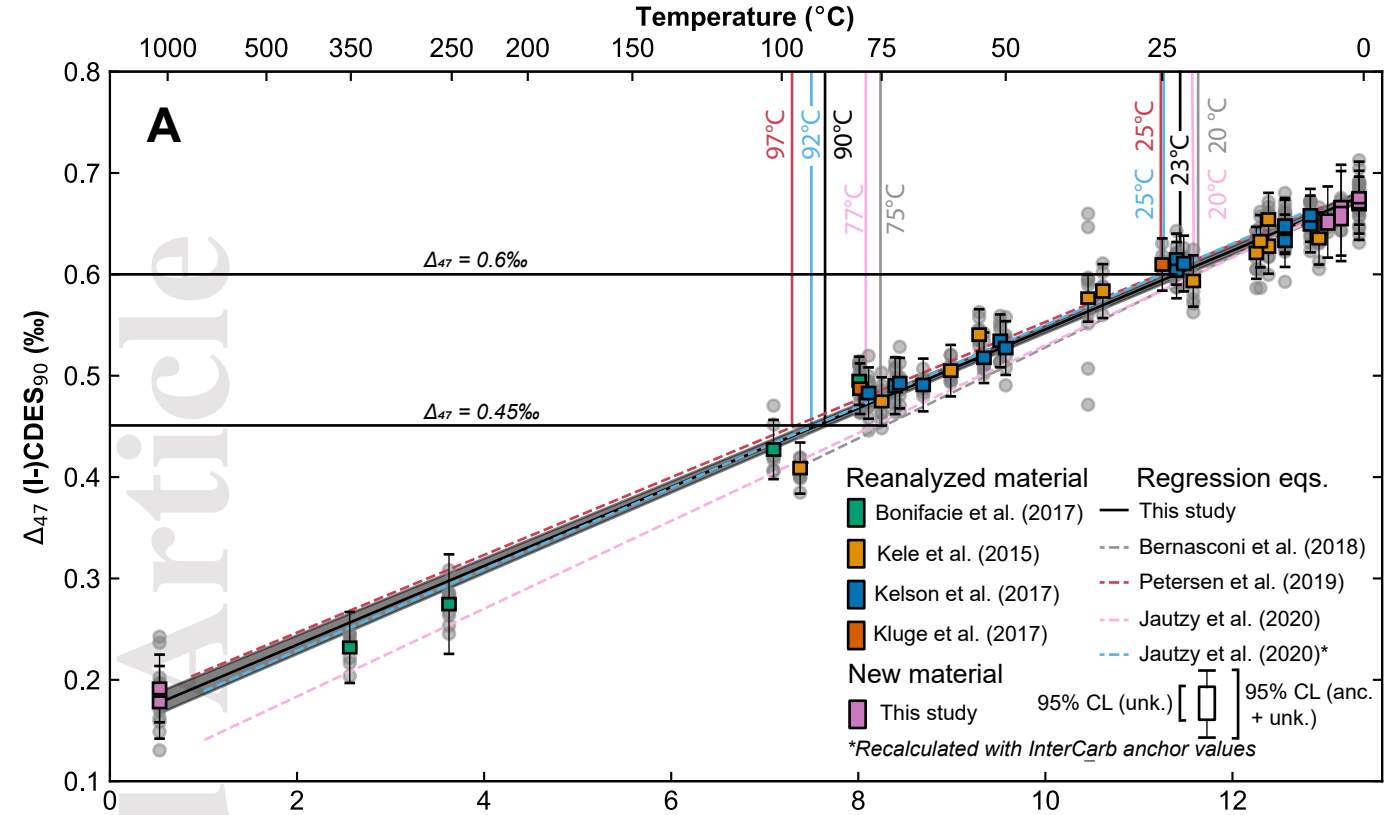
Figure 3. A. All Δ_{47} results from this study shown with data from four recent studies using carbonate-based standardization using laboratory precipitates (Jautzy et al., 2020) and foraminifera (Breitenbach et al., 2018; Peral et al., 2018; Meinicke et al., 2020), recalculated here with InterCarb anchor values (Bernasconi et al., submitted). Error bars correspond to 95% confidence limits accounting for error from both unknown and anchor analyses; boxes correspond to 95% CL not accounting for normalization errors. Regressions through this study (cubic and linear), previous data, and the composite dataset are nearly identical. B. Inset of A from 0–30°C. Slow-growing calcites respectively from Devils Hole, NV, USA, and Laghetto Basso, Italy, measured on an IsoPrime100 at LCSE (see supporting information Text S3) fall directly on the plotted regression lines.

A

$\Delta_{47} = 0 \cdot 0388 \pm 0.0006 \times (10^6/T^2) + 0.156 \pm 0.006$

$\Delta_{47} = 0.0391 \pm 0.0004 \times (10^6/T^2) + 0.153 \pm 0.005$

$\Delta_{47} = 0.039 \pm 0.0004 \times (10^6/T^2) + 0.154 \pm 0.004$

Breitenbach et al. (2018)*   This study
Peral et al. (2018)*   Four prev. studies
Meinicke et al. (2020)*   Composite
Jautzy et al. (2020)*   This study (cubic)
This study   95% CL (unk.)   95% CL (unk. + anc.)

Recalculated with InterCarb anchor values

B

Devils Hole, NV, USA

Laghetto Basso, Italy